

# A Pilot Study Examining the Performance of Polynomial-Modeled Ventricular Shock Electrograms for Rhythm Discrimination in Implantable Devices

JEFFREY L. WILLIAMS, VLADIMIR SHUSTERMAN, and SAMIR SABA

From the Division of Cardiac Electrophysiology, University of Pittsburgh, Pittsburgh, Pennsylvania

**Background:** *Inappropriate shocks continue to be a problem for patients with implantable defibrillators (ICD). We evaluated the performance of polynomial-modeled ventricular electrograms (EGM) to discriminate between supraventricular tachycardia (SVT) and ventricular tachycardia (VT).*

**Methods:** *Seven sets of EGM from patients having both SVT and VT documented during a single ICD interrogation were included. The cardiac cycle was analyzed off-line in two parts, QR and RQ segments, which were modeled separately using third-order and sixth-order polynomial equations, respectively. These segments were then analyzed to determine which polynomial coefficients were most significant for rhythm discrimination.*

**Results:** *When analyzing the QR segment during arrhythmia, there were statistically significant ( $P < 0.05$ ) correlations in 4 of 4 (100%) of the QR coefficients when comparing normal sinus rhythm (NSR) to SVT and 2 of 4 (50%) when comparing NSR to VT or SVT to VT. When analyzing the RQ segment during arrhythmia, there were statistically significant ( $P < 0.05$ ) correlations in 4 of 7 (57%) of the RQ coefficients when comparing NSR to SVT, 5 of 7 (71%) when comparing NSR to VT, and 3 of 7 (43%) when comparing SVT to VT. Using a cutoff value of 50% change from NSR, the ratio of first-order to zero-order QR coefficient was able to completely separate VT from SVT ( $P = 0.03$ ) in this series of patients.*

**Conclusion:** *Our data demonstrate the feasibility of simple polynomial equations that reproduce the depolarization and repolarization phases of human ventricular shock EGM. The ratio of first-order to zero-order QR coefficient was able to reliably discriminate between SVT and VT while reducing the polynomial model to a first-order system. The results of this pilot trial may serve as the basis for a larger prospective trial implementing a discrimination algorithm for use in low computational power implantable devices. (PACE 2006; 29:930-939)*

**defibrillation, ICD, electrophysiology, clinical, computing, electrocardiogram**

## Background

The morphology of the ventricular electrogram (EGM) reflects local<sup>1</sup> and global<sup>2</sup> electrical activity of the heart. There has been a dramatic increase in the utilization of implantable cardioverter defibrillators (ICD) secondary to expanding indications for their use<sup>3,4</sup> and as a result, there is an abundance of EGM information available. The current study first aims to construct a mathematical model of sufficient power to faithfully reproduce the shock (RV tip to can) EGM of the human ventricular EGM. Next, this study evaluates the reproducibility and response of the model during supraventricular (SVT) and ventricular (VT) tachycardias. Finally, the study attempts

to determine which, if any, polynomial coefficients were most significant for rhythm discrimination.

## Methods

### ICD Interrogation and EGM Acquisition

Patients in an ICD registry who underwent routine evaluation in the Device Clinic at the University of Pittsburgh Medical Center had their interrogations retrospectively analyzed. A total of 194 consecutive device interrogations were evaluated and any patient having both SVT and VT on a single interrogation was included. There were no patients who met these criteria that were excluded. A total of six patients having seven episodes of both SVT and VT documented during a single ICD interrogation were included. The EGM data were deidentified prior to analysis.

### Data Acquisition

EGMs obtained during each episode consisted of an atrial bipolar EGM, right ventricular bipolar EGM, and shock (RV tip to can) EGMs. Fifteen to 60 seconds of EGMs were recorded by the ICD depending on the duration of arrhythmia. The

---

This work was supported in part by an ACCF/Merck 2005-2006 Research Fellowship to JLW.

Address for reprints: Jeffrey L. Williams, M.D., Division of Cardiac Electrophysiology, University of Pittsburgh Medical Center, PUH B535, 200 Lothrop Street, Pittsburgh, PA 15213. Fax: 412-647-7979; e-mail: williamsjl4@upmc.edu

Received March 6, 2006; revised April 28, 2006; accepted May 5, 2006.

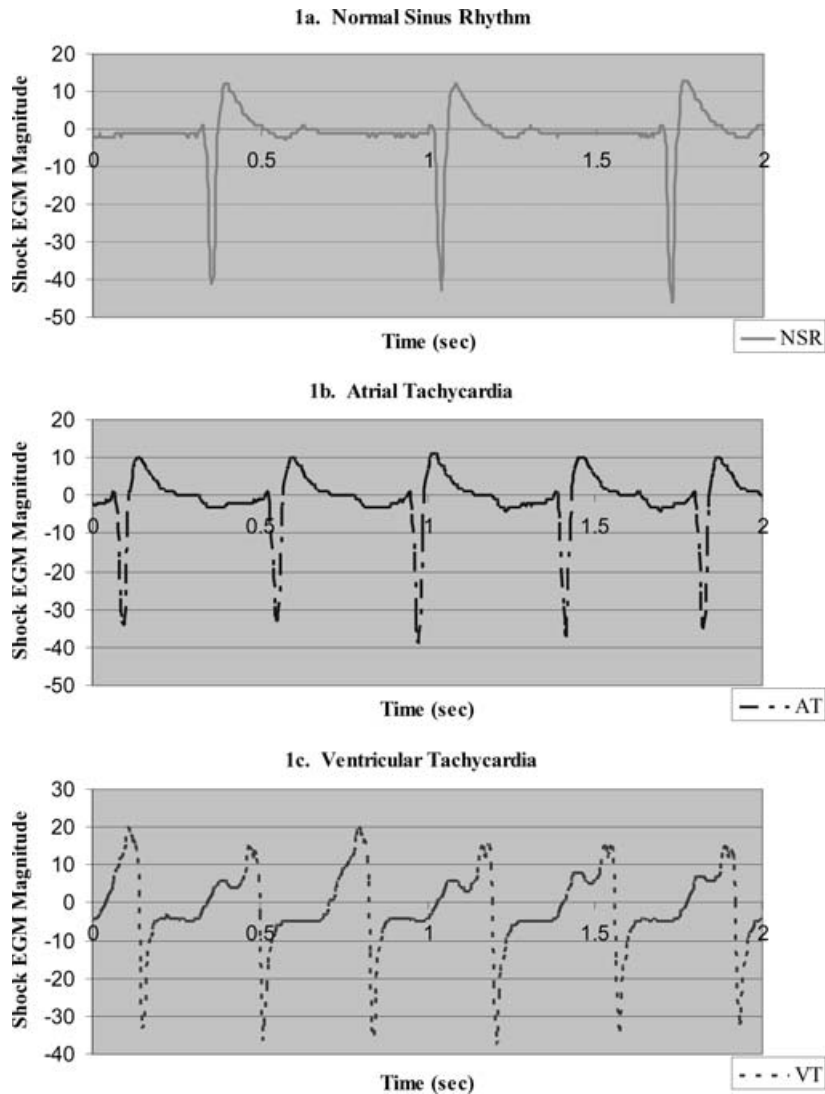


**Figure 1.** A typical patient data set including normal sinus rhythm (A), atrial tachycardia (B), and ventricular tachycardia (C). These shock electrograms represent the raw data that are obtained during ICD interrogation and used for subsequent analysis. The EGMs are sampled at 200 Hz and depicted as a unitless magnitude because the ICD performs a proprietary, fixed scaling prior to storing the waveforms.<sup>28</sup>

sample rate predetermined by the ICD was 200 samples/s.

### Data Analysis and Statistics

The raw data were processed using Matlab (MathWorks, Natick, MA, USA). Figure 1 depicts a typical data set including normal sinus rhythm (NSR, Fig. 1A), SVT, in this case atrial tachycardia (AT, Fig. 1B), and VT (Fig. 1C).

The absolute peak of the QRS wave is the most visually and computationally identifiable component of the EGM. Thus, the identification of this point was chosen as the first step in the signal anal-

ysis and denoted “R” though it may at times represent an S wave. Next, the EGM was divided into two “segments,” the QR and RQ. This segmentation simplifies signal analysis while preserving all the attributes of the original signal. The earliest deflection of the QRS was taken as the onset of the initial segment (QR segment). The initial segment is denoted QR though not all EGMs will contain a Q wave. The peak of the R wave was taken as the end of the QR segment. The second segment, RQ, spans from the peak of the R wave to the earliest onset of the subsequent EGM. The onset of depolarization as evident on the EGM was taken as time zero.

Zero amplitude of the shock EGM corresponds to isoelectric baseline between beats.<sup>5</sup> Thus, the combination of the RQ and QR segments preserves all features of depolarization and repolarization of the original EGM.

A custom Matlab script was used to extract the QR and RQ segments from the ICD interrogation EGM data. The proper segmenting was then visually confirmed and, if needed, adjusted to ensure proper analysis. If it was found that the duration of the QR segment was too short (<15 ms) to allow Matlab's polyfit function to be applied, a splining algorithm was used to increase the sampling frequency while causing no change in the overall duration of the QR segment.

Using Matlab, each QR segment of the processed EGM was then fit to a third-order polynomial equation using the polyfit function ( $f = \text{polyfit}(x,y,n)$ ). Again using Matlab, each RQ segment of the processed EGM was then fit to a sixth-order polynomial equation using the polyfit function ( $f = \text{polyfit}(x,y,n)$ ). This function assigns coefficients to the modeled polynomial  $f(x)$  of degree  $n$  to fit the EGM while minimizing error with a least-squares algorithm. The resulting  $f(x)$  is a row vector of length  $n + 1$  containing the polynomial coefficients in descending powers:

$$f(x) = p_n x^n + p_{n-1} x^{n-1} + \dots + p_1 x + a.$$

Examples of the specific functions (with the corresponding coefficients) used for modeling a representative VT EGM are depicted in Figure 2. The order of the polynomial used to model the segmented EGM was determined by fitting polynomials of increasing order and selecting the model that maximized modeling accuracy while limiting computational complexity. Residuals are the differences between the observed values and the fitted values. In Matlab, both the observed values and modeled values are stored in matrices. The norm of the matrix of residuals is a scalar that quantifies the magnitude of the residuals in that matrix. In general, a smaller norm of the residuals indicates a better model fit. The higher the degree of polynomial chosen the lower the resulting norms of residuals and hence, better model fit. In a prior study,<sup>5</sup> we attempted to balance model order with computational complexity by analyzing the norms of residuals for typical rabbit EGM QR and RQ segments to determine the incremental benefit as higher order polynomials were used. In that study, we empirically limited our model order to the point at which there ceased to be a greater than 20% decrease in the norm of residuals as we increased the model order by one starting with a linear regression. For the baseline QR and RQ segments

analyzed, the sixth-order polynomial was found to be the model at which further increases in order resulted in less than 20% decreases in the norms of residuals. Thus, we were able to maximize modeling accuracy while limiting computational complexity. In this study, a third-order polynomial was found to be the model at which further increases in order resulted in less than 20% decreases in the norms of residuals for the baseline QR segments analyzed. A sixth-order polynomial was found to be the model at which further increases in order resulted in less than 20% decreases in the norms of residuals for the baseline RQ segments analyzed. Figure 2A depicts a sample EGM QR segment during VT fit to a third-order polynomial. Figure 2B depicts a sample EGM RQ segment during VT fit to a sixth-order polynomial.

To assess correlation and reproducibility during a baseline NSR EGM recording, eight consecutive EGM cycles were analyzed. Next, the coefficients of the polynomial model were determined for each of the eight complete cycles of QR and RQ segments. The QR and RQ coefficients of the eight consecutive EGM cycles were first compared using a paired samples *t*-test on SPSS software V10.1.0 (SPSS Inc., Chicago, IL, USA) to assess for baseline correlation of the model coefficients over the recording period. Then, using the methods described by Bland and Altman,<sup>6</sup> the reproducibility of the coefficients was then evaluated using a one-way analysis of variance (ANOVA) for four correlated samples. For this analysis, the null hypothesis ( $H_0$ ) assumes that there is no difference between measured coefficients at the various times over the baseline recording period.

Subsequently, four consecutive EGMs were analyzed at baseline NSR, during SVT, and during VT for each of the patient episodes. The coefficients of the polynomial model were determined for the QR and RQ segments of each of the four cycles. Statistical comparisons between the coefficients (mean  $\pm$  standard deviation) of the segmental, polynomial model during baseline and with each arrhythmia were performed using a two-tailed, paired Student's *t*-test on SPSS software. A *P*-value  $\leq 0.05$  was considered statistically significant.

## Results

### Patient Characteristics

All patients examined in this study were in NSR at baseline. Table I reports the characteristics of each patient episode. The average patient age (mean  $\pm$  standard error) was  $66.3 \pm 6.9$  years and the average left ventricular ejection fraction was  $18.9 \pm 2.3\%$ . Sixty-six percent of patients

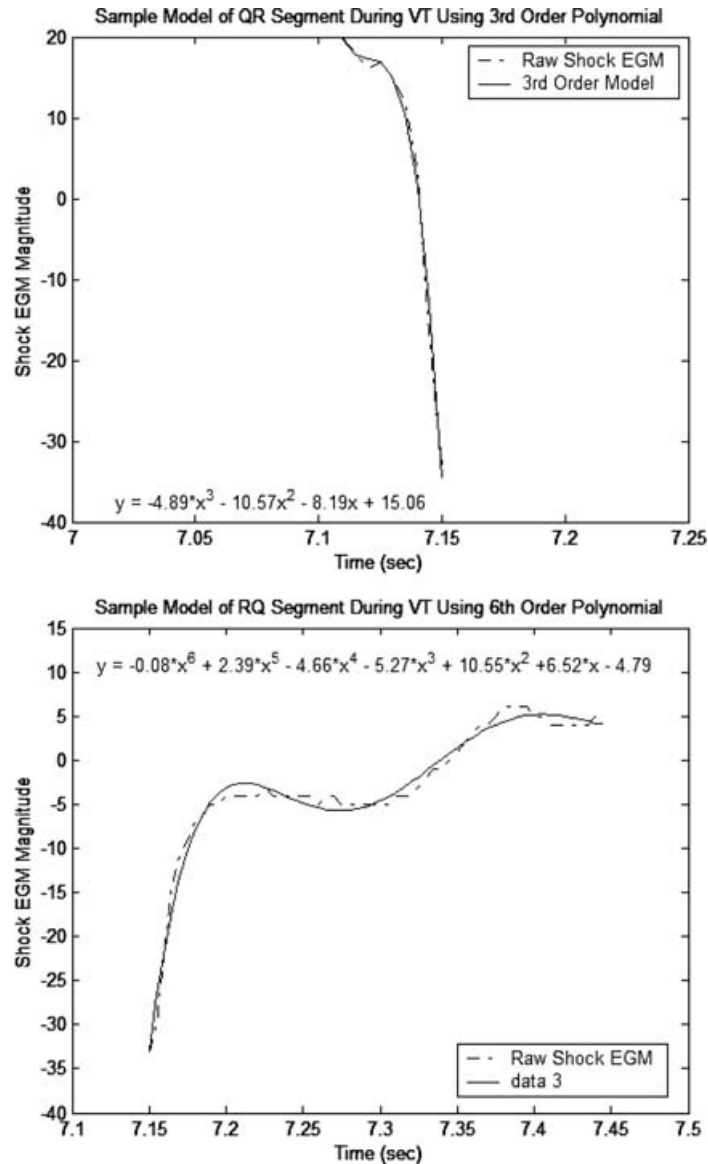


**Figure 2.** (A) Sample EGM QR segment during VT fit to a third-order polynomial. The raw shock EGM was processed as described in the "Methods" section. A third-order polynomial was then fitted to this QR segment. The equation shown in this figure depicts the coefficients that were then used for subsequent analysis. (B) Sample EGM RQ segment during VT fit to a sixth-order polynomial. The raw shock EGM was processed as described in the "Methods" section. A sixth-order polynomial was then fitted to this RQ segment. The equation shown in this figure depicts the coefficients that were then used for subsequent analysis.

had ischemic cardiomyopathy and 57% (4/7 episodes) had a bundle branch block (QRS duration greater than 120 ms). SVT included atrial flutter/fibrillation ( $n = 2$ ), AT ( $n = 3$ ), and AV nodal reentrant tachycardia ( $n = 2$ ). Two of seven SVTs (29%) demonstrated a QRS widening of greater than 30% when compared to sinus rhythm. The ventricular tachycardia was monomorphic in all cases and exhibited a 1:1 atrioventricular relationship in 2 of 7 episodes (29%).

#### Correlation and Reproducibility of the Model

During a baseline NSR EGM recording, the means of the QR and RQ coefficients for the first four consecutive EGMs were compared to the means of the QR and RQ coefficients for the final four consecutive EGMs using a two-tailed, paired samples  $t$ -test. The four coefficients representing the QR segment exhibited a high level of correlation between each set ( $R = 0.999$ ). The seven coefficients representing the RQ segment exhibited

**Table I.**  
Patient Episode Characteristics

Patient	Age	Gender	Device Model	Type of Cardiomyopathy	Ejection Fraction	Sinus Rhythm Cycle Length (ms)	Sinus QRS Duration (ms)	VT Cycle Length (ms)	1:1 AV Relation During VT	SVT Cycle Length (ms)	SVT QRS Duration (ms)
1	49	Male	Guidant 1861	Ischemic	20-25	670	80	360	Yes	320	80
2	55	Male	Guidant 1861	Ischemic	15-20	685	85	370	Yes	460	85
3	73	Male	Guidant 1851	Ischemic	26	1,020	90	360	No	350	105
4	87	Male	Guidant 1861	Ischemic	10-15	715	220	300	No	575	235
5a (Episode 1)	51	Male	Guidant H175	Nonischemic	10-15	520	175	285	No	350	180
5b (Episode 2)	51	Male	Guidant H175	Nonischemic	10-15	520	175	325	No	405	195
6	83	Female	Guidant H170	Nonischemic	20-25	860	155	285	No	855	235

a high level of correlation between each set ( $R = 0.999$ ).

As noted above, the coefficients of the polynomial model were determined for the QR and RQ segments of each of the eight cycles during a baseline NSR EGM recording. After we applied the one-way ANOVA to these repeated measurements, we obtained F-statistics between 0.19 and 6.76 with P-values  $>0.05$  for 7 degrees of freedom. With P-values  $>0.05$ , we have no strong evidence to reject the null hypothesis ( $H_0$ ), which assumes that there is no difference between measured coefficients at the various times over the baseline recording period. Thus, we conclude that our coefficients are reproducible over the baseline NSR recording period.

**Changes in Model Coefficients with Arrhythmias**

Table II depicts the QR model coefficients for NSR, SVT, and VT for each patient episode. Table III depicts the RQ model coefficients for NSR, SVT, and VT for each patient episode. Table IV reports the correlation and significance of the third-order QR model coefficients of all patients when NSR was compared to arrhythmia. When analyzing the QR segment during arrhythmia, there were statistically significant ( $P < 0.05$ ) correlations in 4 of 4 (100%) of the QR coefficients when comparing NSR to SVT and 2 of 4 (50%) when comparing NSR to VT or SVT to VT. Table V reports the correlation and significance of the sixth-order RQ model coefficients of all patients when NSR was compared to arrhythmia. When analyzing the RQ segment during arrhythmia, there were statistically significant ( $P < 0.05$ ) correlations in 4 of 7 (57%) of the RQ coefficients when comparing NSR to SVT, 5 of 7 (71%) when comparing NSR to VT, and 3 of 7 (43%) when comparing SVT to VT.

The lower-order coefficients tended to have a greater significance in this series of patients. We then analyzed the ratio of first-order coefficient ( $p_1$ ) to zero-order coefficient ( $a$ ) in both the QR and RQ models in an attempt to focus on these lower order coefficients and further simplify our algorithm. The ratio of first-order QR coefficient ( $p_1$ ) to zero-order QR coefficient ( $a$ ) is depicted as a percent change in the absolute magnitude from baseline sinus rhythm (NSR) to SVT and VT in Figure 3. Using a cutoff value of 50% change from NSR, the ratio of  $QRp_1$  to  $QRa$  was able to completely separate VT from SVT in these patients. The ratio of first-order RQ coefficient ( $p_1$ ) to zero-order RQ coefficient ( $a$ ) was not predictive.

**Discussion**

This study demonstrated that a segmental polynomial model can reproduce phases of depolarization and repolarization of the human

**Table II.**  
Coefficients (Mean  $\pm$  Standard Deviation) of Third-Order QR Model for Each Patient Episode

	QRp <sub>3</sub>	QRp <sub>2</sub>	QRp <sub>1</sub>	QRa
1 NSR	0.39 $\pm$ 0.79	-7.67 $\pm$ 0.43	-16.25 $\pm$ 2.55	-6.84 $\pm$ 1.18
SVT	-1.45 $\pm$ 1.67	-13.03 $\pm$ 0.93	-20.48 $\pm$ 2.52	-10.10 $\pm$ 0.81
VT	-3.34 $\pm$ 0.58	-14.34 $\pm$ 0.36	-5.18 $\pm$ 1.21	12.08 $\pm$ 0.53
2 NSR	3.21 $\pm$ 0.48	-7.79 $\pm$ 0.75	-22.09 $\pm$ 1.80	-7.76 $\pm$ 0.89
SVT	5.26 $\pm$ 1.42	-3.74 $\pm$ 1.49	-23.05 $\pm$ 3.79	-11.13 $\pm$ 3.18
VT	-3.65 $\pm$ 1.89	-11.03 $\pm$ 0.78	-10.86 $\pm$ 4.59	12.79 $\pm$ 1.86
3 NSR	-5.05 $\pm$ 0.39	2.78 $\pm$ 1.74	33.79 $\pm$ 1.45	28.63 $\pm$ 4.01
SVT	-11.00 $\pm$ 2.78	15.88 $\pm$ 2.74	62.58 $\pm$ 6.94	38.76 $\pm$ 4.01
VT	14.35 $\pm$ 2.29	22.02 $\pm$ 2.11	-10.51 $\pm$ 4.11	-22.35 $\pm$ 3.65
4 NSR	-22.58 $\pm$ 0.88	18.03 $\pm$ 2.94	73.18 $\pm$ 2.45	-27.89 $\pm$ 3.77
SVT	-26.29 $\pm$ 0.75	22.89 $\pm$ 3.24	83.98 $\pm$ 5.42	-39.66 $\pm$ 3.85
VT	-18.97 $\pm$ 2.23	-12.75 $\pm$ 3.28	19.53 $\pm$ 3.77	4.71 $\pm$ 3.58
5a NSR	-1.49 $\pm$ 1.52	1.87 $\pm$ 8.88	25.28 $\pm$ 2.06	28.39 $\pm$ 15.45
SVT	-2.31 $\pm$ 1.13	11.54 $\pm$ 1.15	44.57 $\pm$ 2.64	51.00 $\pm$ 3.58
VT	0.66 $\pm$ 6.46	33.07 $\pm$ 2.34	59.79 $\pm$ 14.08	-58.83 $\pm$ 6.64
5b NSR	-1.49 $\pm$ 1.52	1.87 $\pm$ 8.88	25.28 $\pm$ 2.06	28.39 $\pm$ 15.45
SVT	-4.27 $\pm$ 6.00	14.53 $\pm$ 5.16	50.65 $\pm$ 9.81	41.90 $\pm$ 13.70
VT	-2.57 $\pm$ 2.24	26.18 $\pm$ 1.27	33.46 $\pm$ 7.31	-16.51 $\pm$ 3.63
6 NSR	-0.45 $\pm$ 1.12	3.80 $\pm$ 6.57	14.83 $\pm$ 1.48	12.10 $\pm$ 11.35
SVT	-10.16 $\pm$ 0.41	-2.34 $\pm$ 4.60	51.94 $\pm$ 2.15	51.95 $\pm$ 7.80
VT	0.23 $\pm$ 1.89	20.28 $\pm$ 2.93	31.29 $\pm$ 4.00	3.06 $\pm$ 4.06

ventricular shock EGM while preserving the attributes of the entire EGM at baseline and during SVT and VT. The waveform analysis process allows the EGMs to be modeled with 11 coefficients that are then evaluated for significant changes in magnitude during SVT and VT in the same patients. We derived our model's segmental structure and order based upon preliminary animal studies<sup>7</sup> and then quantified the effects of SVT and VT on these coefficients. The ratio of first-order QR coefficient ( $p_1$ ) to zero-order QR coefficient ( $a$ ) change from NSR was able to completely separate VT from SVT in this small series of patients. In addition, it was able to distinguish SVT from VT in the presence of baseline bundle branch block, 1:1 atrioventricular relationship, and aberrancy during the SVT. A simplified, first-order model of the QR segment may permit implementation into current implantable devices that have limited computing power and potentially provide insight into phases of the cardiac action potential.

### EGM Modeling

Mathematical modeling of the surface electrocardiogram has been shown to be feasible using various methods,<sup>8,9</sup> albeit at the expense of using a large number of coefficients. Correlation

waveform analysis has been used to capture the morphology of ventricular EGM during cardiac arrhythmia and to compare it to the same EGM during normal rhythm.<sup>10-12</sup> These correlation techniques reflect overall morphologic similarity between EGM beats; however, they do not "model" the EGM *per se*. Correlation techniques are not affected by heart rate increases though an increase in amplitude is often seen with increasing sympathetic tone.<sup>13</sup> There are numerous other techniques attempting to discriminate between arrhythmias based on changes in ventricular EGM morphology. Several EGM analyses used the first derivative to assess arrhythmia-induced morphologic feature changes from sinus rhythm.<sup>14-16</sup> Unpublished data from our laboratory demonstrate that wavelet decomposition can reproduce the ventricular EGM quite accurately, albeit with a number of coefficients exceeding 50. Orthogonal expansions such as singular-value decomposition and Karhunen-Loeve transform (principal component analysis) are known to be optimal mathematical solutions to EGM analysis<sup>17-20</sup>; however, this is at a cost of considerable additional computational complexity.<sup>21</sup> In addition, there is controversy surrounding the applicability of ascribing any physiologic significance to the data resulting from such decompositions.<sup>22</sup>

**Table III.**  
Coefficients (Mean  $\pm$  Standard Deviation) of Sixth-Order RQ Model for Each Patient Episode

	<b>RQP<sub>6</sub></b>	<b>RQP<sub>5</sub></b>	<b>RQP<sub>4</sub></b>	<b>RQP<sub>3</sub></b>	<b>RQP<sub>2</sub></b>	<b>RQP<sub>1</sub></b>	<b>RQa</b>
1 NSR	-7.31 $\pm$ 0.39	7.15 $\pm$ 0.30	24.01 $\pm$ 1.46	-20.79 $\pm$ 0.97	-15.38 $\pm$ 1.16	8.84 $\pm$ 0.47	2.54 $\pm$ 0.12
SVT	-2.56 $\pm$ 5.19	10.67 $\pm$ 0.97	8.25 $\pm$ 3.91	-22.76 $\pm$ 2.87	2.20 $\pm$ 3.46	0.21 $\pm$ 1.63	5.50 $\pm$ 0.49
VT	2.59 $\pm$ 0.44	1.63 $\pm$ 0.84	-17.02 $\pm$ 1.32	0.56 $\pm$ 2.90	21.14 $\pm$ 0.43	-3.99 $\pm$ 1.53	0.90 $\pm$ 0.21
2 NSR	-5.99 $\pm$ 0.44	5.54 $\pm$ 0.38	20.68 $\pm$ 1.39	-16.32 $\pm$ 1.03	-15.10 $\pm$ 0.83	7.52 $\pm$ 0.39	0.49 $\pm$ 0.11
SVT	-4.80 $\pm$ 0.40	5.21 $\pm$ 0.41	14.86 $\pm$ 1.39	-12.71 $\pm$ 0.79	-8.75 $\pm$ 1.12	1.85 $\pm$ 0.21	0.19 $\pm$ 0.40
VT	0.13 $\pm$ 0.91	3.34 $\pm$ 1.48	-4.39 $\pm$ 3.52	-7.64 $\pm$ 5.74	9.50 $\pm$ 2.76	8.56 $\pm$ 4.28	-4.38 $\pm$ 0.94
3 NSR	12.23 $\pm$ 0.20	-9.09 $\pm$ 0.32	-45.80 $\pm$ 0.65	28.19 $\pm$ 0.74	39.76 $\pm$ 0.56	-14.55 $\pm$ 0.29	-3.37 $\pm$ 0.07
SVT	-1.05 $\pm$ 1.43	-2.23 $\pm$ 0.81	19.18 $\pm$ 6.07	-15.40 $\pm$ 2.85	-14.42 $\pm$ 6.06	27.46 $\pm$ 1.23	-17.51 $\pm$ 1.79
VT	1.47 $\pm$ 0.47	-3.22 $\pm$ 0.57	1.19 $\pm$ 1.56	0.58 $\pm$ 1.46	-5.72 $\pm$ 0.72	4.05 $\pm$ 0.48	1.74 $\pm$ 0.54
4 NSR	4.74 $\pm$ 0.31	2.92 $\pm$ 0.30	-20.79 $\pm$ 1.32	-17.90 $\pm$ 1.26	35.84 $\pm$ 1.55	14.01 $\pm$ 1.09	-15.19 $\pm$ 0.37
SVT	1.91 $\pm$ 1.87	-2.83 $\pm$ 1.48	-11.48 $\pm$ 8.20	7.80 $\pm$ 6.55	32.92 $\pm$ 9.69	-16.58 $\pm$ 6.86	-16.48 $\pm$ 2.28
VT	4.24 $\pm$ 1.29	-10.84 $\pm$ 0.32	-10.80 $\pm$ 5.82	49.06 $\pm$ 1.77	-23.31 $\pm$ 6.05	-30.59 $\pm$ 2.95	27.55 $\pm$ 1.49
5a NSR	11.71 $\pm$ 0.17	-10.98 $\pm$ 0.73	-34.09 $\pm$ 0.20	27.70 $\pm$ 1.80	6.89 $\pm$ 0.89	-0.44 $\pm$ 0.91	10.89 $\pm$ 0.22
SVT	0.25 $\pm$ 1.19	-13.38 $\pm$ 0.95	25.02 $\pm$ 4.67	15.58 $\pm$ 3.51	-41.39 $\pm$ 4.07	29.52 $\pm$ 2.21	-13.51 $\pm$ 1.74
VT	-1.23 $\pm$ 1.79	-3.39 $\pm$ 1.07	10.36 $\pm$ 7.86	-0.18 $\pm$ 4.35	-24.63 $\pm$ 8.75	-22.57 $\pm$ 4.07	19.08 $\pm$ 2.52
5b NSR	11.71 $\pm$ 0.17	-10.98 $\pm$ 0.73	-34.09 $\pm$ 0.20	27.70 $\pm$ 1.80	6.89 $\pm$ 0.89	-0.44 $\pm$ 0.91	10.89 $\pm$ 0.22
SVT	13.13 $\pm$ 3.44	-19.34 $\pm$ 2.77	-30.38 $\pm$ 14.75	29.69 $\pm$ 8.06	11.49 $\pm$ 10.50	40.07 $\pm$ 3.98	-18.15 $\pm$ 4.66
VT	-4.80 $\pm$ 1.34	0.07 $\pm$ 1.34	29.33 $\pm$ 5.39	-18.64 $\pm$ 4.25	-26.07 $\pm$ 6.10	21.01 $\pm$ 2.80	-6.65 $\pm$ 2.44
6 NSR	7.63 $\pm$ 0.51	-6.42 $\pm$ 0.45	-28.67 $\pm$ 1.76	22.96 $\pm$ 1.24	21.63 $\pm$ 1.39	-14.88 $\pm$ 0.64	0.39 $\pm$ 0.13
SVT	10.40 $\pm$ 0.33	-16.24 $\pm$ 0.42	-26.08 $\pm$ 1.57	44.39 $\pm$ 1.06	1.62 $\pm$ 1.80	-15.16 $\pm$ 1.01	3.90 $\pm$ 0.17
VT	-1.56 $\pm$ 2.34	-1.90 $\pm$ 3.30	12.26 $\pm$ 7.81	-10.41 $\pm$ 11.23	0.40 $\pm$ 5.36	13.43 $\pm$ 7.35	-18.60 $\pm$ 3.38

**Table IV.**

Correlation and Significance of Third-Order QR Model Coefficients During Arrhythmia

		NSR vs SVT	NSR vs VT	SVT vs VT
QRp <sub>3</sub>	Pearson correlation	0.9	0.553	0.361
	P-value	<0.001	0.002	0.059
QRp <sub>2</sub>	Pearson correlation	0.678	0.085	0.339
	P-value	<0.001	0.667	0.078
QRp <sub>1</sub>	Pearson correlation	0.934	0.368	0.446
	P-value	<0.001	0.054	0.017
QRp <sub>a</sub>	Pearson correlation	0.866	-0.668	-0.641
	P-value	<0.001	<0.001	<0.001

**Implementation of the Model in Current Generation of ICDs**

The polynomial model of the human ventricular shock EGM presented here is feasible and reproducible, and may significantly quantify changes in ventricular depolarization and repolarization during arrhythmias. The current automated methods to discriminate SVTs from VTs using existing EGM models and morphologic techniques continue to result in a significant number of inappropriate shocks. A recent study<sup>23</sup> reports that 23–30% of patients are subject to inappropriate shocks. The majority of these inappropriate shocks were due to misclassification of rapidly conducted SVTs. The novel segmentation approach of this model sheds insight into the factors that predispose to ventricular arrhythmias (e.g., changes to the subendocar-

dial action potential) and thus, may afford ICDs a higher specificity for rejecting true supraventricular arrhythmias.

Current ICDs are quite sophisticated but remain limited in computational power and generally consist of an 8-bit microprocessor with a 2.6-MHz clock and 256 kB of memory.<sup>24</sup> This is paltry in comparison to the laptop PC used in this study equipped with a 32-bit microprocessor with a 1.6-GHz clock and 1 GB of memory. The polynomial model (reduced to a first-order system) proposed here may be manageable for ultimate use in computationally limited implantable devices. Thus, using currently available implantable device technology, this model may provide a valuable technique to discriminate between various arrhythmias.

**Table V.**

Correlation and Significance of Sixth-Order RQ Model Coefficients During Arrhythmia

		NSR vs SVT	NSR vs VT	SVT vs VT
RQp <sub>6</sub>	Pearson correlation	0.545	-0.42	-0.594
	P-value	0.003	0.026	0.001
RQp <sub>5</sub>	Pearson correlation	0.84	0.138	0.205
	P-value	<0.001	0.483	0.296
RQp <sub>4</sub>	Pearson correlation	0.201	-0.609	-0.433
	P-value	0.305	0.001	0.021
RQp <sub>3</sub>	Pearson correlation	0.551	-0.489	-0.193
	P-value	0.002	0.008	0.325
RQp <sub>2</sub>	Pearson correlation	0.226	-0.511	-0.043
	P-value	0.247	0.006	0.829
RQp <sub>1</sub>	Pearson correlation	-0.273	-0.5	0.27
	P-value	0.016	0.007	0.165
RQp <sub>a</sub>	Pearson correlation	0.056	-0.370	-0.505
	P-value	0.777	0.052	0.006

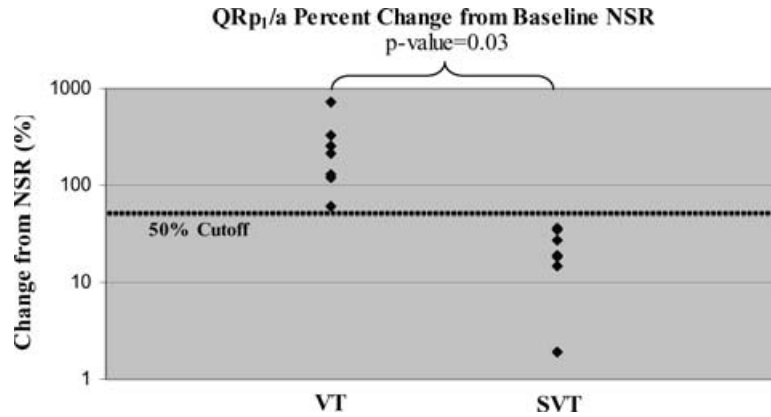


**Figure 3.** The ratio of first-order QR coefficient ( $p_1$ ) to zero-order QR coefficient ( $a$ ) is depicted as a percent change in the absolute magnitude from baseline sinus rhythm (NSR) to SVT and VT. Using a cutoff value of 50% change from NSR, the ratio of  $QRp_1$  to  $QRa$  was able to completely separate VT from SVT in the same patient.

### Limitations of this Study

There are several limitations to the data presented here. First, the ICD has a predetermined sampling frequency of 200 samples/s. Thus, our frequency bandwidth is limited to at most half of the sampling frequency or 100 samples/s. This is well above the “frequency-of-interest” range used in other research on human EGM analysis which is typically in the range of 1–44 samples/s (or Hz).<sup>25</sup> There is a caveat, however, in that VT EGMs have slightly more prominent high-frequency components<sup>26</sup> when compared to NSR beats.

Second, in this study, we attempted to balance model order with computational complexity by analyzing the norms of residuals for ventricular shock EGM QR and RQ segments to determine the incremental benefit as higher order polynomials were used. However, it is obvious from Figure 2 that the model is not a perfect fit to the raw data. Given the QR model’s ability to distinguish SVT from VT under a variety of confounding factors (e.g., preexisting bundle branch block, aberrancy, and 1:1 atrioventricular relationship), it is unclear if balancing model order with complexity has decreased our discrimination sensitivity.

Third, the physiologic significance of each order coefficient in our model remains to be elucidated. The goal of this study was discrimination of SVT from VT using ventricular EGMs available from ICDs; thus, attaching a physiologic significance to each coefficient was not studied. Therefore, we cannot conclusively explain the predictive nature of the QR-segment coefficients and the inability of the RQ-segment coefficients to differentiate SVT from VT.

Finally, it is very much possible that the relationship between percentage change in  $QRp_1/a$

may be a chance observation; however, this ratio was able to discriminate between SVT and VT with a P-value of 0.03. A prospective analysis of this discrimination technique on larger numbers of patients experiencing both SVTs and VTs is needed.

### Conclusion

This study demonstrated that a polynomial model of the human ventricular shock EGM is feasible, reproducible, and can reliably discriminate supraventricular from ventricular arrhythmias. Ventricular EGMs may not have long-term stability.<sup>15,27,28</sup> Therefore, one could look at a change in coefficients rather than absolute value. Heuristic featuring leads to information loss, whereas sample-based featuring is more appropriate.<sup>26</sup> Hence, modeling the system using its baseline features will minimize information loss.

The development of an EGM model may ultimately enable detailed analysis of medication effects, arrhythmias, and arrhythmic substrates by examining the changes in the model with various interventions. These data may provide a valuable technique to quantify cardiac ion channel function through the analysis of EGMs. Long-term applications of this new method may include incorporating it into cardiac devices such as pacemakers and defibrillators where the ventricular EGMs can be used to monitor physiologic changes ranging from ischemia to electrolyte disturbances and to provide a new tool to quantify the action of antiarrhythmic medications and assess cardiac ion channel function. In addition, similar modeling techniques can be applied to EGMs from other cardiac chambers, namely the atria, to provide a more complete picture of the electrical status of the heart.

## References

- Muzikant AL, Hsu EW, Wolf PD, Henriquez CS. Region specific modeling of cardiac muscle: Comparison of simulated and experimental potentials. *Ann Biomed Eng* 2002; 30:867–883.
- Aslanidi OV, Clayton RH, Lambert JL, Holden AV. Dynamical and cellular electrophysiological mechanisms of ECG changes during ischemia. *J Theor Biol* 2005; 237:369–381.
- Moss AJ, Zareba W, Hall WJ, et al. Prophylactic implantation of a defibrillator in patients with myocardial infarction and reduced ejection fraction. *N Engl J Med* 2002; 346:877–883.
- Bardy GH, Lee KL, Mark DB, et al. Amiodarone or an implantable cardioverter-defibrillator for congestive heart failure. *N Engl J Med* 2005; 352:225–237.
- Esler J. 2006. Personal Communication, Guidant Corp., St. Paul, MN.
- Bland JM, Altman DG. Statistical methods for assessing agreement between two methods of clinical measurement. *Lancet* 1986; 1:307–310.
- Williams JL, Shusterman V, Saba S. A segmental polynomial model of ventricular electrograms as a simple and efficient morphology discriminator for implantable devices. *Ann Noninvasive Electrocardiol*, 2006; 11:271–280.
- Mukhopadhyay S, Sircar P. Parametric modelling of ECG signal. *Med Biol Eng Comput* 1996; 34:171–174.
- Dingfei G, Srinivasan N, Krishnan SM: Cardiac arrhythmia classification using autoregressive modeling. *BioMed Eng OnLine* 2002; 1:1–12.
- Finelli CJ. The time-sequenced adaptive filter for analysis of cardiac arrhythmias in intraventricular electrograms. *IEEE Trans Biomed Eng* 1996; 43:811–819.
- DiCarlo LA, Jenkins JM, Winston SA, Kriegler C. Differentiation of ventricular tachycardia from ventricular fibrillation using intraventricular electrogram morphology. *Am J Cardiol* 1992; 70:820–822.
- Stevenson SA, Jenkins JM, DiCarlo LA. Analysis of the intraventricular electrogram for differentiation of distinct monomorphic ventricular arrhythmias. *Pacing Clin Electrophysiol* 1997; 20:2730–2738.
- Finelli CJ, DiCarlo LA, Jenkins JM, Winston SA, Li P-C. Effects of increased heart rate and sympathetic tone on intraventricular electrogram morphology. *Am J Cardiol* 1991; 68:1321–1328.
- Davies DW, Wainwright RJ, Tooley MA, Lloyd D, Nathan AW, Spurrell RAJ, Camm AJ. Detection of pathological tachycardia by analysis of electrogram morphology. *Pacing Clin Electrophysiol* 1986; 9:200–208.
- Throne RD, Jenkins JM, DiCarlo LA. A comparison of four new time-domain techniques for discriminating monomorphic ventricular tachycardia from sinus rhythm using ventricular waveform morphology. *IEEE Trans Biomed Eng* 1991; 38:561–570.
- Gold MR, Hsu W, Marcovecchio AF, Olsovsky MR, Lang DJ, Shorofsky SR. A new defibrillator discrimination algorithm utilizing electrogram morphology analysis. *Pacing Clin Electrophysiol* 1999; 22:179–182.
- Lux RL. Karhunen-Loeve representation of ECG data. *J Electrocardiol* 1992; 25:195–198.
- Laguna P, Garcia J, Roncal I, Wagner G, Lander P, Mark R. Model-based estimation of cardiovascular repolarization features: Ischaemia detection and PTCA monitoring. *J Med Eng Technol* 1998; 22:64–72.
- Garcia J, Lander P, Sornmo L, Olmos S, Wagner G, Laguna P. Comparative study of local and Karhunen-Loeve-based ST-T indexes in recordings from human subjects with induced myocardial ischemia. *Comput Biomed Res* 1998; 31:272–292.
- Laguna P, Moody GB, Garcia J, Goldberger AL, Mark RG. Analysis of the ST-T complex of the electrocardiogram using the Karhunen-Loeve transform: Adaptive monitoring and alternans detection. *Med Biol Eng Comput* 1999; 37:175–189.
- Coggins RJ, Jabri MA. A low-complexity intracardiac electrogram compression algorithm. *IEEE Trans Biomed Eng* 1999; 46:82–91.
- Lamothe R, Stroink G. Orthogonal expansions: Their applicability to signal extraction in electrophysiological mapping data. *Med Biol Eng Comput* 1991; 29:522–528.
- Sweeney MO, Wathen MS, Volosin K, Abdalla I, DeGroot PJ, Otterness MF, Stark AJ. Appropriate and inappropriate ventricular therapies, quality of life, and mortality among primary and secondary prevention implantable cardioverter defibrillator patients: Results from the Pacing Fast VT Reduces Shock Therapies (PainFREE Rx II) Trial. *Circulation* 2005; 111:2898–2905.
- Graves-Calhoun A. 2005. Personal Communication, Medtronic Inc., Minneapolis, MN.
- Paul VE, O’Nunain S, Malik M, Camm AJ. Temporal electrogram analysis: Algorithm development. *Pacing Clin Electrophysiol* 1990; 13:1943–1947.
- Rojo-Alvarez JL, Arenal-Maiz A, Artes-Rodriguez A. Discriminating between supraventricular and ventricular tachycardias from EGM onset analysis. *IEEE Eng Med Bio* 2002; January-February, 16–26.
- Hook BG, Achlinski FE. Value of ventricular electrogram recording in the diagnosis of arrhythmias precipitating electrical device shock therapy. *J Am Coll Cardiol* 1991; 17:985–990.
- Barold HS, Newby KH, Tomassoni G, Kearney M, Brandon J, Natale A. Prospective evaluation of new and old criteria to discriminate between supraventricular and ventricular tachycardia in implantable defibrillators. *Pacing Clin Electrophysiol* 1998; 21:1347–1355.